Miniaturized 2.4 GHz Antenna and Path Loss Investigations for Metal Containers Monitoring

Brahim Fady, Gunter Vermeeren, Wout Joseph, *Senior Member, IEEE*, Mustapha Benjillali, *Senior Member, IEEE*, Abdelwahed Tribak, *Member, IEEE*, Emmeric Tanghe, Luc Martens, *Member, IEEE*

***Abstract*—This paper presents a future terminal antenna to enhance the performance of wireless container monitoring systems. It first introduces an optimized design that is experimentally validated for Wireless Personal Area Network (WPAN) technology taking into account the harsh environment of containers. The proposed antenna exhibits excellent performance next to the container in terms of return loss, gain, and bandwidth. Further, deterministic and stochastic path loss models for inter-container link budget calculations are used to illustrate the impact of the optimized antenna on path loss and attainable maximum ranges.**

***Index Terms*—Container, path loss, link budget, optimized antenna, ISM band, Internet of things.**

I. Introduction

The evolving trend in industry chain process is to improve distribution services. Sensor networks, low-power microcontrollers and optimized antennas are increasingly used in supply chain. The clients need accurate information (e.g, location, arriving time, temperature) on the whereabouts of their containers, anywhere enroute to ensure the integrity and the security of the transported goods. The port and the ship presents difficult radio frequency issues (attenuation, reflexion, interference) caused by the metallic structure of the container which impacts the antenna reflection, gain and propagation (e.g., shielding and interference of signals [1]). However, the communication still can be improved using optimal antennas.

Path loss models for container environments have been proposed in [1] and [2], but they are based on non-optimized antennas next containers. Propagation for container environments has been investigated scarcely up to now. Based on measurements, path models in a container terminal are proposed for the frequency band [1 GHz, 4 GHz] using different antenna heights [2]. In [1], intra- and inter-container path loss for shipping container monitoring systems is investigated for IEEE 802.15.4 (433, 868, and 2400 MHz) and extra-container path loss is examined at GSM/UMTS (900, 1850, and 2100 MHz).

The iMinds-COMACOD project is co-funded by iMinds, a research institute founded by the Flemish Government and Companies. This research is also partly funded by the Fund for Scientific Research - Flanders (FWO-V, Belgium) project G.0325.11N. W. Joseph and E. Tanghe are Post-Doctoral Fellow of the FWO-V (Research Foundation - Flanders).

B. Fady, G. Vermeeren, W. Joseph, E. Tanghe, L. Martens are with iMinds-INTEC-Ugent (Department of Information Technology - Ghent University), Gaston Crommenlaan 8 box 201, B-9050 Ghent, Belgium.

M. Benjillali is with the Communication Systems Department, INPT, Rabat, Morocco.

A. Tribak is with the Microwave and Communication Antenna Subsystems Department, INPT, Rabat, Morocco.

E-mail: Wout.joseph@intec.ugent.be

The objective is to design an optimal antenna attached to a metal container for operation in the 2.4 GHz industrial, scientific and medical (ISM) wireless communication band. Based on the proposed design, the link budget is considerably improved. This will enable connecting containers to the internet and reducing the costs of containers monitoring systems.

II. Proposed antenna design

A. Optimization Setup

We started from a planar off-the-shelf antenna (RHEA dual band antenna 2.4 GHz/5.8 GHz), in order to obtain a low-cost antenna (q.v Figure 2). The substrate of the RHEA antenna sizes 50x16x1 mm^3 and modeled as a dielectric with a relative permittivity $\epsilon_r = 5$. The dipole is fed asymmetrically with one arm sized 2x21 mm^2 and the other 2x22 mm^2. Both arms are modeled as perfect electric conductors (PECs). We optimized this antenna near the container, modeled as PEC and sized 2377x5682x2377 mm^3, using the full genetic algorithm (GA) optimization routine on top of the 3D finite-difference time-domain (FDTD) method as implemented in the software platform SEMCAD-X (SPEAG, Zurich, Switzerland).

Figure 1 shows the antenna mounted on the inner rail of the container. The antenna is placed at 23 mm from the metal surface of the container. For safety reasons, and to avoid vandalism, the antenna is located inside the housing of the circuitry, called the air-ventilator box. Besides the antenna, the air-ventilator box contains two printed circuit boards (PCBs), a GPS and a GPRS/GSM board. Each board measures 38x75x1.6 mm^3 and modeled as PEC. The GPRS/GSM board denoted as "Bottom PCB" is placed at the bottom of the air-ventilator whereas the GPS Board, denoted as "Top PCB", is placed on top of the GPRS/GSM board with a separation of 4 mm.

The parameters of the optimization are the length of the dipole arms, the width of the arms and the separation (step of 2 mm) between the antenna and the container surface. In the optimization process, we took into account the container as well as the PCBs and the ventilator box.

B. Final Design

Figure 2 shows the manufactured design, tuned taking into account the estimated relative permittivity of the substrate, the holder and the cover. The resulting dimensions of the planar dipole are 22x2 mm^2 for each arm. The gap between the arms is 1 mm. The substrate made of FR4 material has a relative permittivity of 4.4, and sizes 8x53x0.8 mm^3. The soldering spaces are modeled as PEC surfaces sizing 2x4 mm.

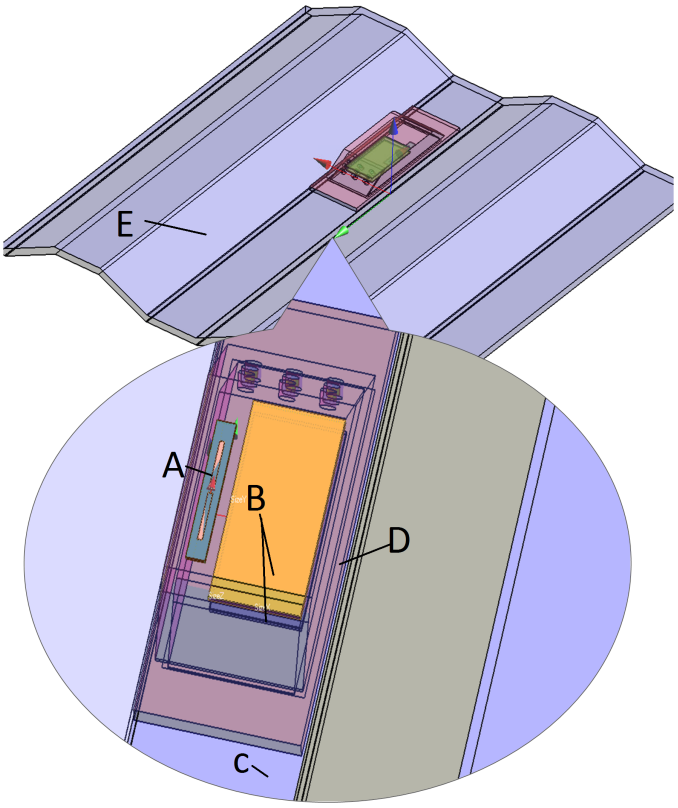

Figure 1. Configuration of the antenna on the container. A: antenna placed upside-down, B: Top PCB and Bottom PCB, C: inner rail of container, D: air-ventilator box, E: a part of the container.

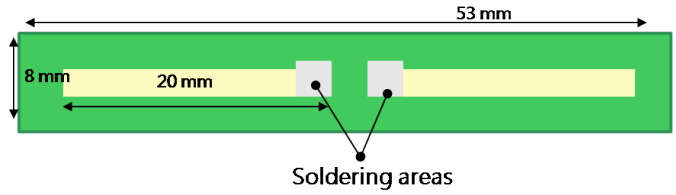

Figure 2. The final design tuned near container.

C. Measurement and Simulation Results

1) Comparison in Free Space : Figure 3 describes and compares the results of simulations to measurements in free space in terms of S_{11} with respect to 50 Ω. We observe that in free space, the measurements correspond to simulations with a small offset in the resonant frequency up to 0.1 GHz. We note also that the bandwidth measured is 0.2 GHz less than simulation results.

2) Next to Metal Plate: Figure 4 shows the measured S_{11} near a metal plate. We observe that both simulated and measured S_{11} cover the ISM radio band at 2.4 GHz. The measurements show that the bandwidth increases with decreasing width of the dipole arms. We have to remark that the measurements were performed in our testlab where fading could not be avoided. Figure 4 also shows that the optimized antennas performs up to 15 dB better in terms of S_{11} in the 2.4 GHz band compared with the off-the-shelf antenna (RHEA dual band antenna 2.4 GHz/5.8 GHz), which is clearly detuned (to 2.15 GHz) when operated next to the metal plate.

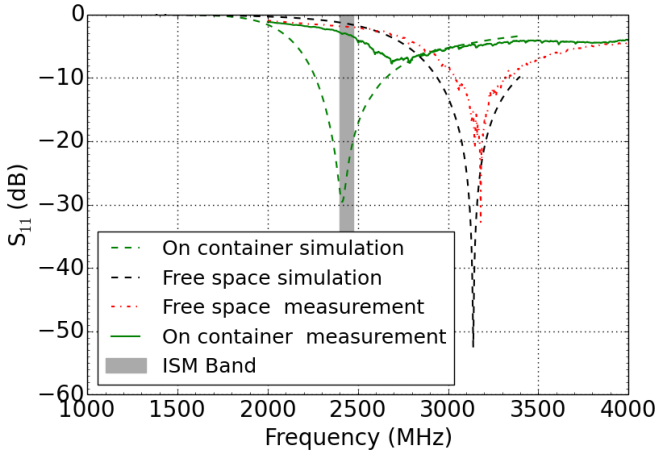

Figure 3. Free space comparison between simulation and measurements of the S_{11} parameter.

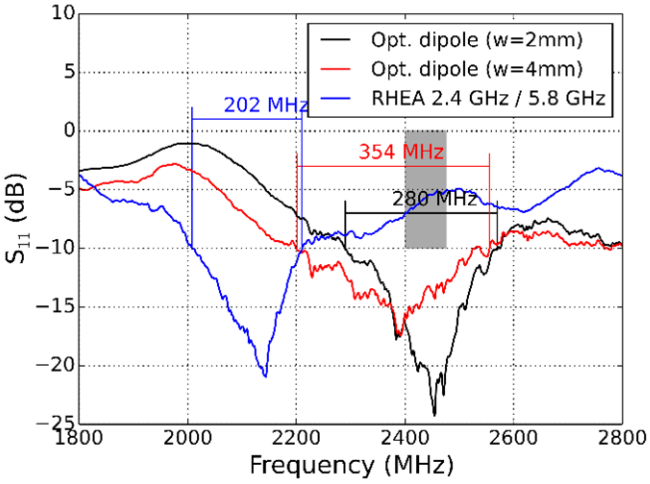

Figure 4. S_{11} measurements on a metal plate and influence of the width of the dipole arms on the reflection.

3) Antenna Mounted on The Container: Finally, we also measured reflection and transmission of the optimized antenna on the container. Figure 6 shows the measured reflection on a container. Both dipole antennas cover the ISM band at 2.4 GHz.

4) Estimation of The Relative Permittivity of The Substrate, Holder and Cover: The dielectric properties of the plastics of the cover and the holder were unknown in advance, whereas we selected for the substrate of the antenna a typical value of FR4 $\epsilon_r = 4.9$.

To estimate the relative permittivity of the holder, we measured on a metal plate in our testlab, the reflection of the antenna mounted on the holder as shown in Figure 7 (b), and compared it with simulations (same configuration) while varying the relative permittivity of the holder in simulations (cf. Figure 8). We obtained a resonance frequency same as the measurement for $\epsilon_r = 1.5$. In the same way we evaluated the relative permittivity of the cover. The configuration is shown in Figure 7 (a), the antenna is mounted on the holder and ceiled with the cover. The simulations fit to measurements, in term of resonance frequency, for $\epsilon_r = 1.8$.

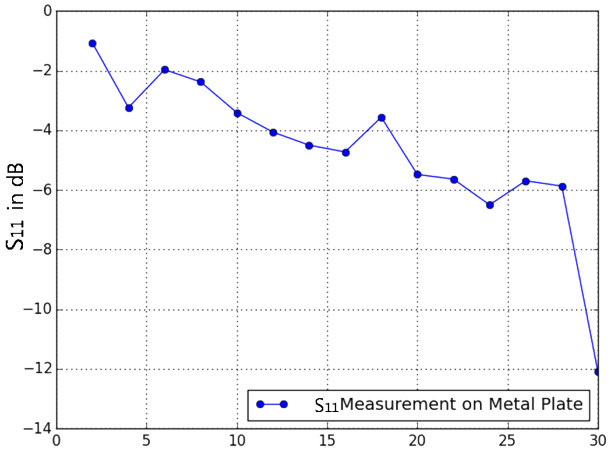

Figure 5. Metal impact on the RHEA antenna reflection at 2.4 GHz.

Figure 6. S_{11} of the optimized antennas on the container.

5) Investigating the Influence of External Factors on The Antenna: Figure 8 shows the influence of the holder and the cover on S_{11}, and compares it with the simulation results. The measured S_{11} of the antenna attached to the holder on the metal plate, Figure 7 (a), shows a resonance frequency of 2.95 GHz, but the simulated S_{11}, with the same configuration with selected permittivity, resonate at 2.7 GHz. In the same figure, we observe that when adding the cover, the measured S_{11} of the antenna resonates at 2.7 GHz, otherwise the S_{11} simulation result, using the selected permittivities, resonate at 2.4 GHz. This comparison allowed us to estimate the relative permittivity of the holder and the cover (q.v in the previous subsection).

6) Investigating the Influence of the PCBs: After investigating the influence of the cover, we shed light in this part on the influence of the PCBs. The lower PCB is located at the surface of the metal plate (inner rail of the container), thus it has no additional effect on the antenna besides the influence of metal plate in terms of reflection. Hence, we describe in this part only the influence of the Top PCB, which is 5.6 mm separated from the surface of the inner rail.

The Figure 9 shows a comparison between the S_{11} result of the model without the top PCB and the result when including the Top PCB Module. We observe that in the absence of the top PCB, the antenna radiates in the ISM band at 2.4 GHz with a S_{11} up to -30 dB. On the other hand, when adding the top PCB, the value of resonance frequency nearby changes (a shift of 0.2 MHz), otherwise the reflection coefficient increases to -14 dB. This means that the top PCB degrades the quality of the antenna (increases the reflection) and makes the optimization of the new design more difficult.

III. Channel Model and Link Budget

After designing an optimized antenna near container accounting for external factors, we characterize in this section the path loss in order to provide a channel model that can be used, for further research, in a container environment. Finally

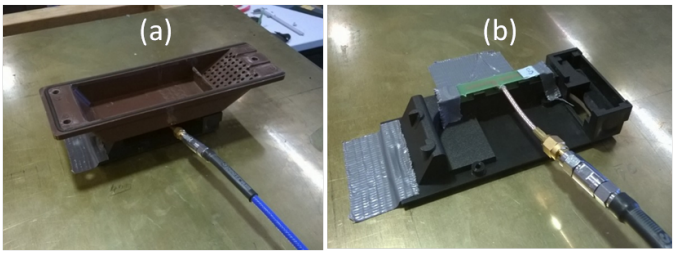

Figure 7. Influence of the holder and the cover of the Track4C node on the reflection of the planar dipole antenna

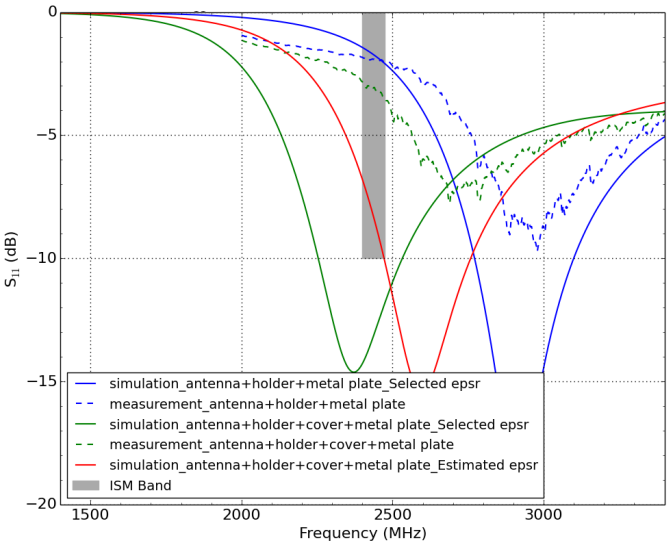

Figure 8. (a) : Antenna attached to the holder. (b) : The antenna is ceiled with cover of the air-ventilator.

we will calculate the coverage range,based on the link budget, of the tuned antenna.

A. Path Loss

1) Excluding Antenna Gain: Path loss (P_L) is the reduction in power density of the transmitted signal (wave) [8]. Path loss P_L is used for the link budget calculations of a telecommunication system. The power at the receiver input terminals, P_r, can be expressed as :

$$P_r = \frac{P_t G_r G_t}{P_L L_t L_r} \Rightarrow P_L = \frac{P_t G_r G_t}{P_r L_t L_r} \quad (1)$$

Where P_r is the received power and P_t is the emitted power. G_t, G_r are the gains of the receiver and the transmitter antennas, respectively. L_t,L_r are feeders losses.

2) Including Antenna Gain: Similarly to a Wireless Body Area Network (WBAN), where the human body affects the antenna radiation pattern, the metallic structure of the container makes the dipole antenna not omnidirective. Thereby, the antenna effect cannot be removed from the propagation path loss [1][7]. By this way, the path loss used in WBAN studies PL_{incl} includes the antenna effect and differs thus from P_L:

$$PL_{incl} = \frac{P_L L_t L_r}{G_r G_t} = \frac{P_t}{P_r} \quad (2)$$

Henceforth, we refer by path loss to PL_{incl}.

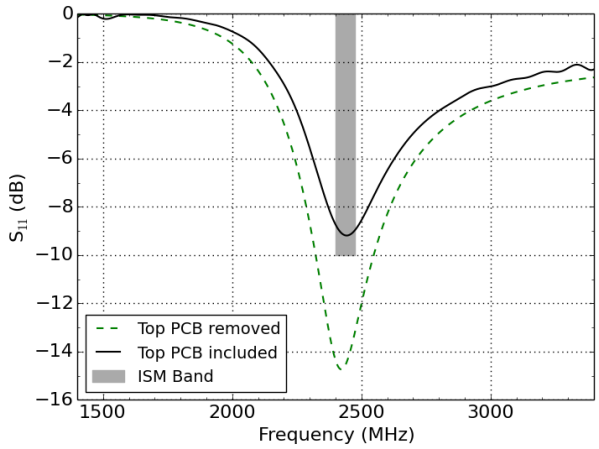

Figure 9. S_{11} result and comparison between Top PCB included and not included

B. Propagation Result of The Optimized Design

We investigate in this part the transmission in terms of S_{21} along a metal plate and a container using the optimized design. First, we compare the measurements to simulations of the propagation, and we end comparing the non-optimized design with tuned design in terms of transmission.

The measurement of the path loss, in terms of the scattering parameter S_{21}, along a single container consisted of the antenna placed on the holder which was attached to the inner rail of the container (Figure 10). The transmitter and the receiver antennas were both connected to the vector network analyzer (VNA) which is a Rohde Schwarz ZNB20. During these measurements, we had to remove the cover to be able to connect the antenna to the VNA.

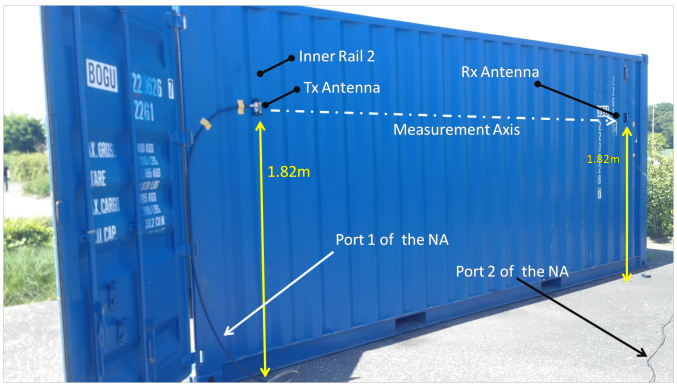

Figure 10. configuration of the S_{21} measurement on the container

Figure 11 shows the S_{21} measurements performed on the container. We selected the two antennas with the best S_{11} performance on the container. We placed the Tx antenna in the second inner rail of the container, and we moved the Rx antenna through the rest of inner rails of the container. In Figure 11, we observe that the S_{21} result of the measurement is much better than the simulation result where the S_{21} decreases swiftly and monotonically. This is due to the absence of the multipath effect in the simulation compared to the environment of measurements where the multipath is ensured by the object around the container. With respect to the simulation result the fluctuations are not prominent but the S_{21} decreases rapidly. We observe that the measured S_{21} decreases slowly but undergoes fluctuations. One of the main reasons of these fluctuations is the obstruction caused by the rails of the container. For both simulation and measurement we can notice the influence of the container which degrades the propagation performance of the antenna (decreasing the S_{21} and shadowing effect).

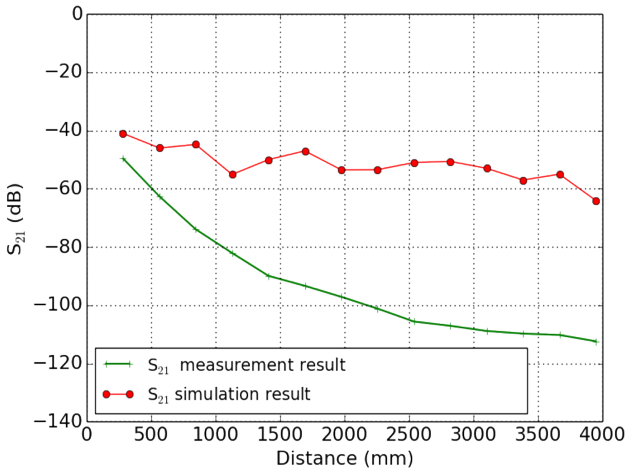

Figure 11. The measured S_{21} along a single container using the optimized antenna.

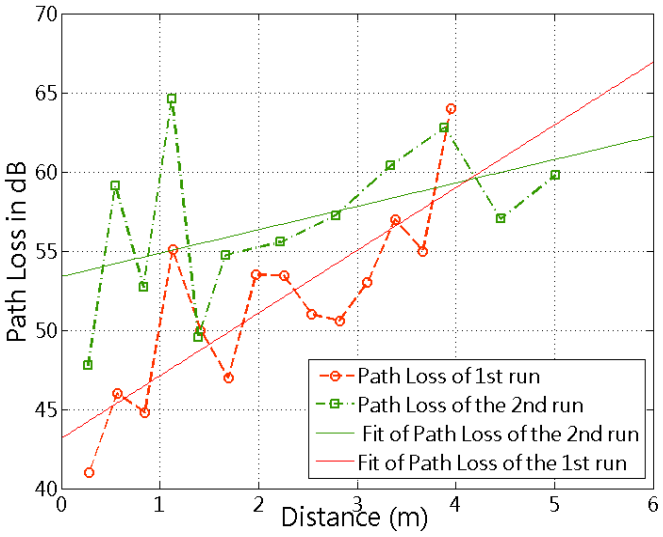

Figure 12. Comparison of measured PL on the container between the non-optimized antenna and the final design.

Figure 12 compares the non-optimized design(RHEA antenna) and the final design in term of measured transmission (path loss) between two nodes along the container for a separation step of up to 280 mm. For both designs, we clearly observe the fading of the environment resulting in a non-monotonic decrease of S_{21} with separation between the two nodes. For a distance lower than 4 meters, the RHEA design exhibits better transmission (about 6 dB in average) than the

optimized antennas (optimized design). However, the path loss expressed by the first run design increases rapidly (already up 60 dB at 4 m) for separations (between transmitter and receiver) higher than 4 meters.

C. Link Budget

1) General: The container path loss model [1] consist of a power decreasing term and of two stochastic terms.

$$PL_{incl} = b_0 + b_1 d + \chi_s + \chi_f \quad (3)$$

Where b_0 and b_1 are regression parameters from the deterministic part of the model and (χ_s,χ_f) represent the stochastic part. The random variable χ_s expresses the random fluctuations of path loss originating from the shadowing of physical objects in the wireless channel (called shadow fading). The random variable χ_f, so-called fast fading margin, results from the random fluctuations of the path loss due to changes over time in the layout of the container channel. The measurement step was higher than the wavelength, thus we will not account for the fast fading margin in the link budget calculation ($\chi_f = 0dB$).

2) Calculation of Regression Parameters and Shadow Fading Margin: To calculate the shadow fading margin, we consider a 2.4 GHz WPAN system for communication between containers [2], Data transmission rates vary around 250 kilobits/second in the 2.4 GHz frequency band. WPAN nodes can sleep most of the time, thus the average power consumption can be low. Transmission distances range from 10 to 100 m line-of-sight, depending on power output and environmental characteristics. The system sensitivity is -108 dBm with a maximum transmission power of up to 24 dBm. As discussed before, the measurements were carried on the container using identical antennas (optimized design), cf. Figure 10. The transmitter is placed inside the air-ventilation box and the receivers are moved in steps of 282 mm along the inner-rails of the container. Based on sample data resulting in 16 records, and thus considering that the random data fluctuation is T-distributed, the shadowing margin calculated at the 95% confidence bounds is 3.02 dB.

3) Calculation of Maximum Range: In this part, we investigate the attainable range for the tuned antenna and compare it to the attainable range allowed by the first run design (not tuned). The tracking devices/sensors, used for containers monitoring, have minimum accepted received power of $-94\ dBm$ at 2.4 GHz. The extracted gain of the first run antenna at the direction of measurement is 1.2 dBi, and it is of up to 2 dBi for the design. Taking into account the fade margin (2.45 dB), we extract the maximum range using the following link budget:

$$PL = b_0 + b_1 d + \chi_s + \chi_f \leq PL_{max}, PL_{max} = 94\ dB. \quad (4)$$

In Table 1 we compare the maximum ranges of the non-optimized and the optimized design. The maximum range of the optimized design is 30 m higher than the non-optimized design. This enables us to obtain larger ranges and thus less devices are needed; resulting in a reduced cost (accounting for millions of container).

Terminal antenna	freq. [GHz]	Gain [dBi]	Max. Range [m]
Non-optimized antenna	2.4	2	11
Optimized antenna	2.4	11	41

Table I
MAXIMUM RANGE COMPARISON BETWEEN THE NON-OPTIMIZED DESIGN AND THE OPTIMIZED ANTENNA

IV. CONCLUSIONS

In this paper, we have designed an optimal WPAN antenna next to the metal container that takes into account the impact of the ventilator box, the tracking circuit, and the feeding cable. We investigated the most adequate orientation and position in which the antenna can be deployed. The optimized model, with a return loss equal to -22 dB and a gain of up to 11 dBi, produces a path loss of up to 18 dB lower than for non-optimized design. The ranges increase from 18 m to 41 m using the optimized system, which reduces the cost of deployment.

REFERENCES

[1] E. Tanghe, W. Joseph, P. Ruckebusch, L. Martens, and I. Moerman, *"Intra-, Inter-, and Extra-Container Path Loss for Shipping Container Monitoring Systems"*, IEEE Antennas and Wireless Propag. Letters, Vol. 11, 2012, pp 2–3.

[2] R. J. Katulski, J. Sadowski, and J. Stefanski, *"Propagation path loss modeling in container terminal environment"*. in Proc. 68th IEEE Veh. Technol. Conf. (VTC-Fall), Calgary, AB, Canada, Sep. 2008, pp 1–4.

[3] S. J. Ambroziak, R. J. Katulski, *"On the usefulness of selected radio waves propagation models for designing mobile wireless systems in container terminal environment"*, in Proc 30th URSI Gen. Assembly Sci. Symp., Istanbul, Turkey, Aug. 2011, pp. 3–4.

[4] F. Molisch, *"Ultrawideband Propagation Channels-Theory, Measurement, and Modeling"*, IEEE Trans. on Vehi. Tech., vol. 54, September 2005, pp 1–5

[5] C. Xiaohua and X. Hanbin, *"Propagation prediction model and performance analysis of RFID system under metallic container production circumstance"*, Microelectron. J., vol. 42, pp 247–252, 2011.

[6] A. Balanis, *"Advanced engineering electromagnetics"*, John Wiley Month Sons, Inc., New York, 1989.

[7] Parini, M. R. Kamarudin, T. Z. Salim, D. T. M. Hee, R. Dubrovka, A. S. Owadally, W. Song, A. Serra, P. Nepa, M. Gallo, and M. Bozzetti, *"Antennas and propagation for on-body communication systems" IEEE*, Antennas Propag. Mag., vol. 49, no. 3, pp 41–58, Jun. 2007.

[8] S. Stavrou, S. Saunders, *"Factors influencing outdoor to indoor radio wave propagation" in Proc. 12th Int. Conf. Antennas Propag.*, London, U.K., Mar. 2003, pp 581–585.